oriented would produce the observed seismic signals. This is a much weaker requirement than the one suggested in (*20*), where even at zero temperature the whole single crystal (100%) has to be oriented with one of its axes along the spin axis of the planet. In passing, we note that bcc velocities (Table 1) are a better match to the seismic velocities in Earth's center [11.26 km/s (*18*)] than are hcp velocities.

Recently, it was suggested that the IC consists of two parts; the central part seems to possess an anisotropy different from the rest of the core (*7*). Later, it was proposed that the innermost IC (IMIC) is elastically less anisotropic (*8*). Such a different elastic behavior can be explained in terms of two iron phases, one of which (bcc) is anisotropic and the other (hcp) isotropic. If the *PT* slope of the hcp-bcc boundary and the geotherm in the core cross each other, then the different elastic behavior might be explained by the bcc-hcp phase transition, where the outer anisotropic part of the IC consists of the anisotropic bcc phase and the IMIC consists of a mixture of bcc and hcp iron alloys. The exact position of the hcp-bcc alloy *PT* boundary is unknown. However, if the field of the bcc stability is narrow (and it most likely is), then such a transition is probable. An alternative explanation could be that during the formation of the IMIC, the processes responsible for the formation of a lattice preferred orientation were weaker, and therefore in this part of the core a random orientation of bcc crystals is dominant. In either case, the bcc phase is an indisputable favorite over the hcp phase to be responsible for the anisotropy of the IC. This is strong evidence for the presence of a bcc iron/iron alloy phase in Earth's inner core.

References and Notes

1. A. Morelli, A. M. Dziewonski, J. H. Woodhouse, *Geophys. Res. Lett.* **13**, 1545 (1986).
2. K. C. Creager, *Nature* **356**, 309 (1992).
3. I. Lehmann, *Bur. Cent. Seismol. Int.* **14**, 3 (1936).
4. A. Cao, B. Romanowicz, *Geophys. Res. Lett.* **34**, L08303 (2007).
5. A. Souriau, B. Romanowicz, *Phys. Earth Planet. Inter.* **101**, 33 (1997).
6. X. Song, D. V. Helmberger, *J. Geophys. Res.* **100**, 9805 (1995).
7. M. Ishii, A. Dziewonski, *Proc. Natl. Acad. Sci. U.S.A.* **99**, 14026 (2002).
8. C. Beghein, J. Trampert, *Science* **299**, 552 (2003).
9. B. Romanowicz, X.-D. Li, J. Durek, *Science* **274**, 963 (1996).
10. S. Karato, *Science* **262**, 1708 (1993).
11. M. I. Bergman, *Nature* **389**, 60 (1997).
12. S. Yoshida, I. Sumita, M. Kumazawa, *J. Phys. Condens. Matter* **10**, 11215 (1998).
13. B. A. Buffett, *Science* **288**, 2007 (2000).
14. S. C. Singh, M. A. J. Taylor, J. P. Montagner, *Science* **287**, 2471 (2000).
15. B. A. Buffett, H.-R. Wenk, *Nature* **413**, 60 (2001).
16. E. Birch, *J. Geophys. Res.* **57**, 227 (1952).
17. L. V. Altshuler, K. K. Krupnikov, B. N. Ledenev, V. I. Zhuchikhin, M. I. Brazhnik, *Zhur. Eksp. Teor. Fiz.* **34**, 874 (1958).
18. A. M. Dziewonski, D. L. Anderson, *Phys. Earth Planet. Inter.* **25**, 297 (1981).
19. R. J. Hemley, H.-K. Mao, *Int. Geol. Rev.* **43**, 1 (2001).
20. L. Stixrude, R. E. Cohen, *Science* **267**, 1972 (1995).
21. We are aware of a paper (*33*) that claims to solve the problem we deal with in our paper. The authors (*33*) reported a computationally obtained anomalous change of *c/a* ratio (*c* is the size of the hexagonal unit cell along the [001] direction, and *a* is the corresponding size in the [100] and [010] directions on the basal plane; all atoms occupy identical positions when *c/a* = 1.6299, the so-called ideal ratio) in hexagonal iron on increasing temperature. That could save the hexagonal phase as the IC material. However, one of the authors of that paper (*33*) has recently published another paper (*34*) on the same subject, where it is demonstrated that the result in the previous publication (*33*) is an artifact of erroneous calculations. Therefore, we do not discuss those results in our paper.
22. A. B. Belonoshko, R. Ahuja, B. Johansson, *Nature* **424**, 1032 (2003).
23. C. Gannarelli, D. Alfé, M. J. Gillan, *Phys. Earth Planet. Inter.* **152**, 67 (2005).
24. J. M. Brown, R. G. McQueen, *J. Geophys. Res.* **91**, 7485 (1986).
25. M. Ross, D. A. Young, R. J. Grover, *J. Geophys. Res.* **95**, 21713 (1990).
26. M. Matsui, O. L. Anderson, *Phys. Earth Planet. Inter.* **103**, 55 (1997).
27. L. Vočadlo *et al.*, *Nature* **424**, 536 (2003).
28. L. Dubrovinsky *et al.*, *Science* **316**, 1880 (2007).
29. A. B. Belonoshko, R. Ahuja, B. Johansson, *Phys. Rev. Lett.* **84**, 3638 (2000).
30. L. Koci, A. B. Belonoshko, R. Ahuja, *Phys. Rev. B* **73**, 224113 (2006).
31. A. B. Belonoshko, E. I. Isaev, N. V. Skorodumova, B. Johansson, *Phys. Rev. B* **74**, 214102 (2006).
32. A. B. Belonoshko *et al.*, *Science* **316**, 1603 (2007).
33. G. Steinle-Neumann, R. E. Cohen, L. Stixrude, O. Gulseren, *Nature* **413**, 57 (2001).
34. X. W. Sha, R. E. Cohen, *Phys. Rev. B* **74**, 064103 (2006).

35. We thank B. Smith and I. Todorov for the DL_POLY package and K. Kadau for the package MD_render. Computations were performed at the Parallel Computer Center (PDC) in Stockholm, the National Supercomputing Center in Linköping, and Los Alamos National Laboratory (New Mexico, USA). Supported by the Swedish Research Council and the Swedish Foundation of Strategic Research.

10 September 2007; accepted 20 December 2007
10.1126/science.1150302

The Spatial Pattern and Mechanisms of Heat-Content Change in the North Atlantic

M. Susan Lozier,[1]* Susan Leadbetter,[2] Richard G. Williams,[2]* Vassil Roussenov,[2] Mark S. C. Reed,[1] Nathan J. Moore[1]†

The total heat gained by the North Atlantic Ocean over the past 50 years is equivalent to a basinwide increase in the flux of heat across the ocean surface of 0.4 ± 0.05 watts per square meter. We show, however, that this basin has not warmed uniformly: Although the tropics and subtropics have warmed, the subpolar ocean has cooled. These regional differences require local surface heat flux changes (±4 watts per square meter) much larger than the basinwide average. Model investigations show that these regional differences can be explained by large-scale, decadal variability in wind and buoyancy forcing as measured by the North Atlantic Oscillation index. Whether the overall heat gain is due to anthropogenic warming is difficult to confirm because strong natural variability in this ocean basin is potentially masking such input at the present time.

Recent evidence that the world's oceans have warmed over the past 50 years (*1*, *2*), with the attendant increase in the ocean's heat content an order of magnitude larger than the increase in the atmospheric and cryospheric heat content (*2*, *3*), has underscored the importance of the ocean as a heat reservoir for Earth's climate system. To facilitate predictions of future oceanic heat uptake, however, an understanding of how the ocean has warmed in response to long-term natural and/or anthropogenic forcing is important. A mechanistic understanding of this warming, the goal of this study, begins with an examination of the spatial variability of the observed warming, followed by modeling experiments designed to isolate the mechanisms responsible for the observed pattern. This study focuses on the North Atlantic, a basin with strong, documented climate variability (*4*–*8*) as well as unparalleled data density (*9*).

To establish the spatial pattern of heat-content change in the North Atlantic, we analyzed historical hydrographic station data from the National Oceanic Data Center World Ocean Database 2005 (*10*). Temperature data from 1950 to 2000 were binned into 2° horizontal grids for 11 constant depth layers spanning the sea surface to the ocean floor. The constraints imposed by data density and our choice of 2° spatial resolution restricted our analysis of temporal change to two time periods, 1950 to 1970 and 1980 to 2000 (fig. S1). Thus, we determine whether the ocean's heat content at

[1]Division of Earth and Ocean Sciences, Nicholas School of the Environment and Earth Science, Duke University, Durham, NC 27708, USA. [2]Department of Earth and Ocean Sciences, Liverpool University, Liverpool L69 3GP, UK.

*To whom correspondence should be addressed. E-mail: mslozier@duke.edu (M.S.L.); ric@liverpool.ac.uk (R.G.W.)
†Present address: Department of Geography, Michigan State University, East Lansing, MI 48823, USA.

Downloaded from www.sciencemag.org on February 8, 2008

the end of the 20th century was significantly different from what it was near the mid-century mark.

The integration of the 11 temperature layers leads to a significant heat-content gain for the basin as a whole [$1.610 \times 10^{22} \pm 0.19 \times 10^{22}$ J (SE); table S1] that compares relatively well to an earlier analysis of basin-integrated change (*1*). This heat-content gain between the two 20-year periods, primarily concentrated in the upper 2 km, requires an equivalent surface heat influx of 0.42 ± 0.05 W m^{-2} over the entire North Atlantic. A striking pattern to the heat-content change in the North Atlantic over the past 50 years (Fig. 1A) reveals that this basin has not experienced a uniform warming trend. Although the subtropics and tropics show an overall gain, the subpolar region has experienced a significant loss (table S1). Regional heat-content changes can be as large as $\pm 1.5 \times 10^{20}$ J between the two 20-year periods (Fig. 1A), changes that would have required a surface heat flux increase of about ±4 W m^{-2} from the former to the latter time period, an estimate that is an order of magnitude larger than the basin-averaged heat flux of 0.42 ± 0.05 W m^{-2}.

To explore mechanisms responsible for the observed North Atlantic heat-content changes, we conducted a modeling study. The ocean model experiments were run with the use of a well-documented ocean general circulation model (*11*) with 1.4° horizontal resolution spun up from rest with climatological monthly forcing fields and then integrated by using realistic surface forcing fields, winds, and buoyancy over the time period from 1950 to 2000. Given the uncertainty in surface forcing fields, all model experiments were run with reanalysis products from two agencies: European Centre for Medium-Range Weather Forecasts (ECMWF) (*12*) and National Center for Environmental Prediction and National Center for Atmospheric Research (NCEP/NCAR) (*13*). Because the products yielded qualitatively similar results, NCEP/NCAR-forced model results are shown as Supporting Online Material (SOM) figures. To test the model's skill at reproducing the observed heat-content changes, we used model temperature data from two 20-year model integrations, one from 1950 to 1970 and another from 1980 to 2000, to compute the modeled heat-content changes from the latter time period to the former. For both sets of forcing fields, there is a heat-content gain over the tropics and much of the subtropical gyre, yet a heat loss over the subpolar gyre (Fig. 2A and fig. S3A), a pattern broadly reflective of the observed fields (Fig. 1A), including a clear subtropical-subpolar gyre boundary separating the regions of heat gain and loss. There are differences, however, with the model integrations gaining insufficient heat over the Sargasso Sea and retaining more heat over the western side of the tropics, as well as having a loss of heat along 24°N, compared with the data. Another important difference is that the modeled heat-content changes are generally of larger amplitude than the observed changes (table S1). It is unclear whether this difference results from the inherent

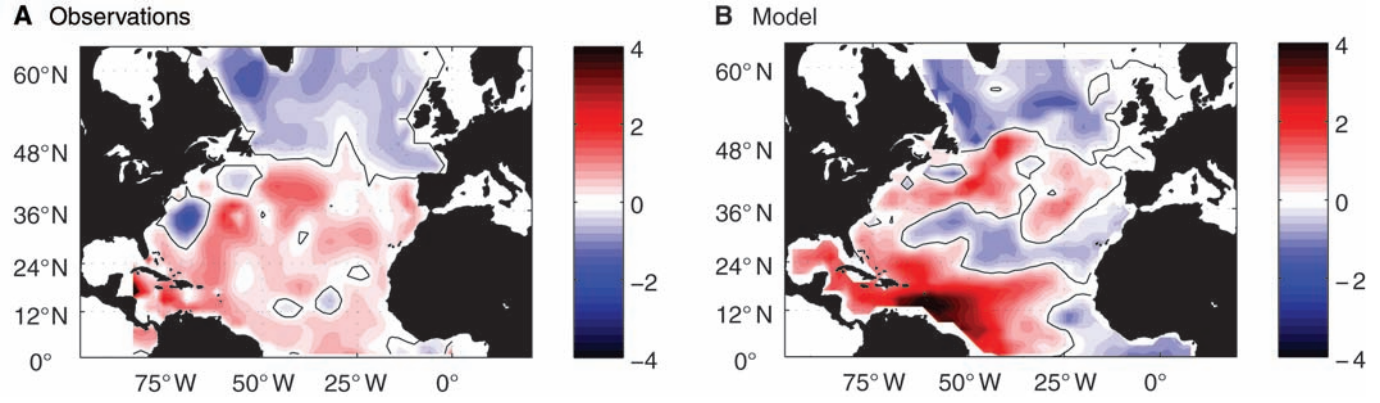

Fig. 1. Change in ocean heat content (color bar indicates units of 10^{20} J; red represents a gain in heat for the later period) between the 20-year periods 1950–1970 and 1980–2000 diagnosed from (**A**) historical data integrated over the water column and (**B**) 1.4° ocean model output using realistic ECMWF wind and buoyancy forcing after a 60-year spin-up. Observations and model data were binned onto the same 2° grid. The observations reveal an overall gain in heat in the tropics and subtropics and a loss of heat in the subpolar ocean.

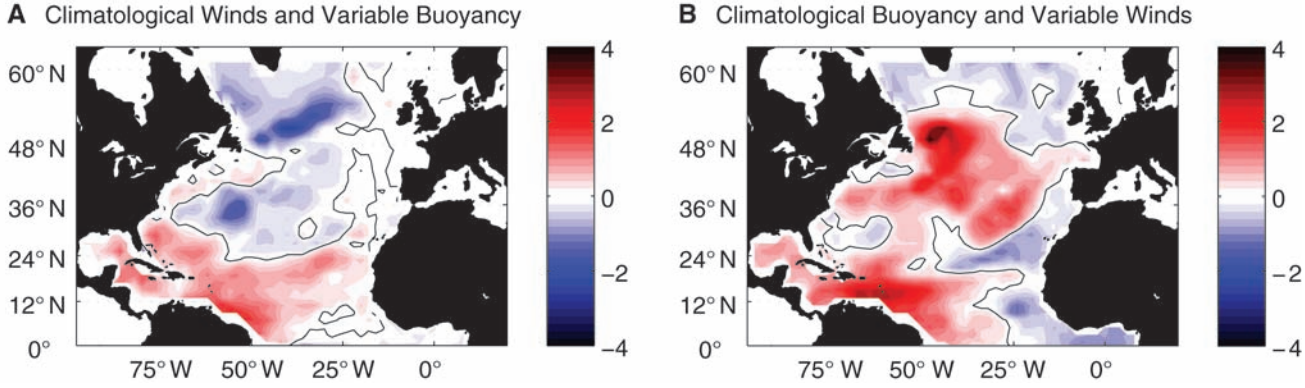

Fig. 2. Change in ocean heat content (color bar indicates 10^{20} J; red represents a gain in heat for the later period) between the 20-year periods 1950–1970 and 1980–2000 diagnosed from idealized model experiments (**A**) using realistic surface buoyancy fluxes from ECMWF, but with climatological winds, and (**B**) using realistic winds from ECMWF, but with climatological surface buoyancy fluxes. Because the ECMWF reanalysis product is available from 1958 only, the ECMWF study uses reconstructed 1950–1957 forcing from the average of 1958–1970. For this comparison, two 20-year integrations were conducted: one with forcing from 1950 to 1970 and another with forcing from 1980 to 2000. In order to separate the mechanical and thermal effects of the wind, we forced the variable-wind runs with climatological latent and sensible heat fluxes.

Downloaded from www.sciencemag.org on February 8, 2008

smoothing that results from the use of hydrographic data irregularly distributed in space and time and/or whether the difference results from a poor knowledge of heat and freshwater fluxes and boundary conditions for the model. Lastly, we note that the broad pattern of heat-content change remained unaltered when the same modeling experiments were repeated at 0.5° horizontal grid spacing (fig. S3B).

Given the broad correspondence between the large-scale patterns of heat content from the model and the data, we investigated the extent to which these patterns are controlled either by surface buoyancy fluxes or by wind-induced circulation changes. First, the model experiments were repeated with the same surface heat and freshwater fluxes described above but with climatological winds. In this case (Fig. 2A), the model integrations again lead to a gain in heat content over the tropics and a loss over the subpolar gyre, but this loss of heat extends unrealistically over the central part of the subtropical gyre, a clear mismatch with the observations. In a second experiment, the model was forced by climatological surface heat and freshwater fluxes, but with realistic winds. In this opposing case, the gain in heat content extends over the tropics and much of the subtropical gyre, but there is insufficient loss of heat over the subpolar gyre (Fig. 2B). From these two model experiments, we conclude that the gain in heat content over the tropics and loss over the subpolar gyre is a consequence of changes in air-sea heat and freshwater fluxes, whereas the gain in heat content over the subtropical gyre is primarily a consequence of wind-induced circulation changes.

The distinction in forcing mechanisms for the subtropical and subpolar regions seen in the model is largely consistent with observations: Analyses of temperature and salinity data have revealed that changes in the subpolar gyre are a reflection of density-compensated water-mass changes, whereas the subtropical changes are due to the deepening of density surfaces,

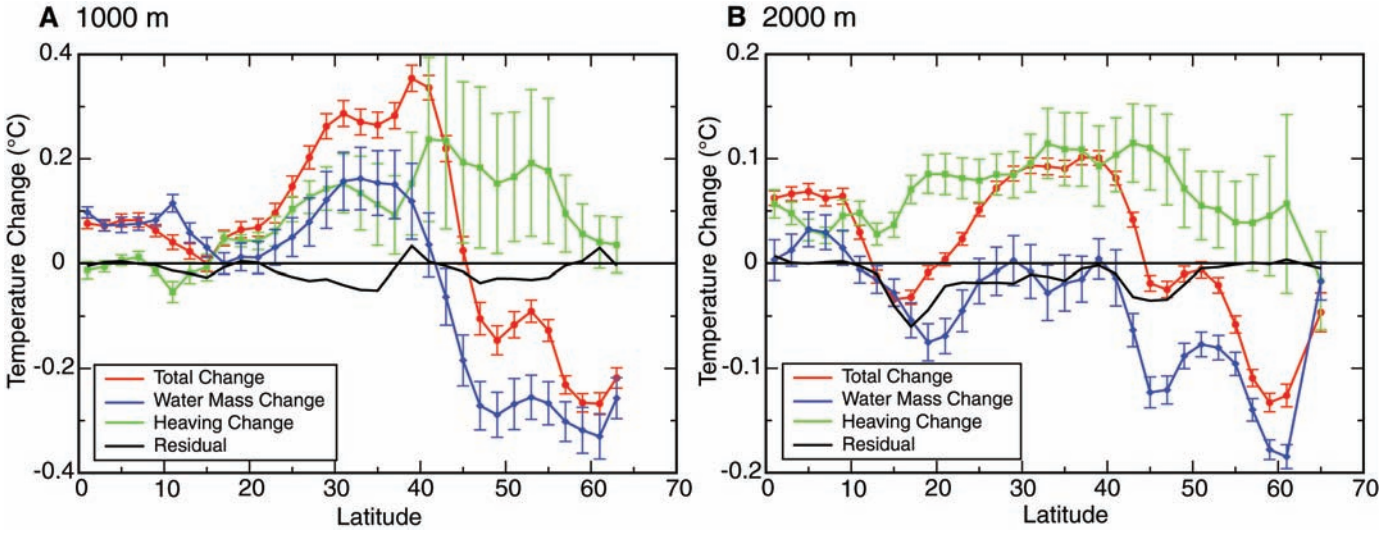

Fig. 3. Observed zonally averaged temperature change (°C) between the 20-year periods 1950–1970 and 1980–2000 along a constant depth (red) of (**A**) 1000 m or (**B**) 2000 m, revealing a warming in the tropics and subtropics but a cooling north of 45°N. This temperature change at constant depth is separated into changes along an isopycnal (blue) and the temperature change from a deepening of isopycnals (green) and a residual from the misfit of these independent estimates (black). Over the whole basin, there is a warming from the deepening of isopycnals (heave, green), which is opposed by a cooling of the water mass along the isopycnals (blue) in the subpolar gyre. The vertical displacement of the isopycnals is related to changes in the wind forcing. Error bars indicate standard errors.

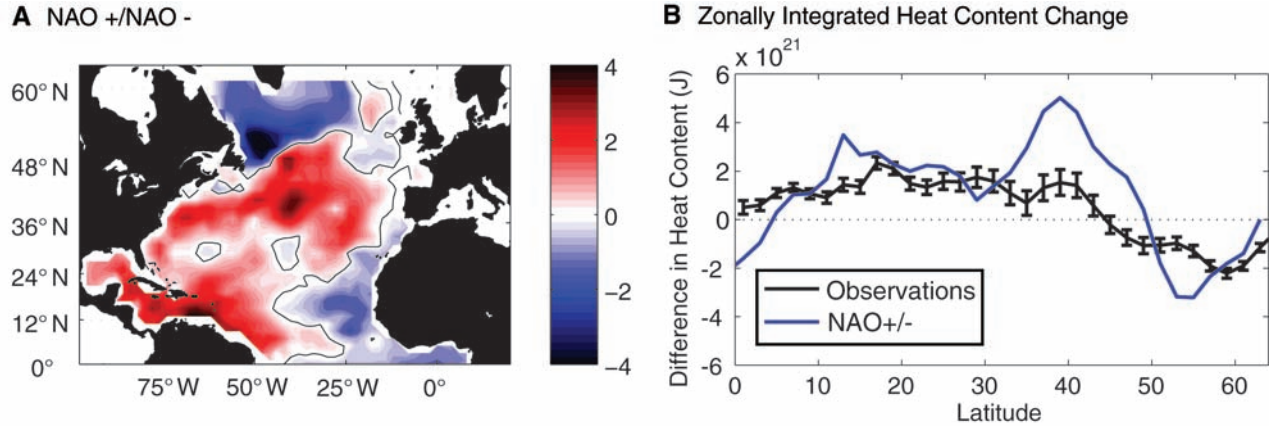

Fig. 4. (**A**) Change in ocean heat content (color bar indicates 10^{20}]; red is a gain) from a model run using NAO– composite forcing to a model run using NAO+ composite forcing. (**B**) Zonal integral in heat-content change for the observations (black; error bars represent standard errors) and for the NAO model runs (blue). Sixteen years were averaged to create a composite NAO– index of –2.34; 20 years were averaged to create a composite NAO+ index of 2.37. Model integrations were also made in which the NAO+ composite forcing was defined as the forcing fields of the 5 individual years with the most positive NAO indices over the 50-year record, randomly ordered, and then repeatedly integrated for 20 years; a NAO– state was similarly defined. Model results were similar to those shown above.

Downloaded from www.sciencemag.org on February 8, 2008

in agreement with a past study that analyzed differences from repeated hydrographic cross sections (*4*). A decomposition of the total temperature change (*14*, *15*) at a particular depth into that which is created by temperature change along a surface of constant density, attributable to water mass change, and that which is created when isotherms move vertically past a depth horizon, attributable generally to wind-forced displacement or heaving, reveals this gyre-specific response (Fig. 3). In the subpolar gyre, the cooling at both 1000 m (the base of the thermocline) and 2000 m (representative of the deep waters below the thermocline) results from colder waters residing on the density surfaces at those depths, suggesting that water-mass changes play a dominant role. In contrast, for the subtropical gyre there is a more complicated response, with the warming at 2000 m due to a deepening of isotherms and the warming at 1000 m due to both a deepening of isotherms and water-mass changes. Ironically, this simple, basinwide decomposition of temperature change over the past 50 years reveals a complexity that requires a more nuanced explanation than simple basinwide warming.

These observations of temperature changes compare well with the model results: An analysis of model output reveals that the wind-induced increase in heat content over the subtropical gyre is achieved through a redistribution of heat associated with an enhanced wind-induced pumping down of the thermocline and an increased northward transport of heat from the tropics to the northern subtropical gyre. This interpretation of how the subtropical warming is largely controlled is also supported from a comparison of hydrographic sections along 36°N conducted in 1959, 1981, and 2005. Similar heave/water-mass diagnostics applied to these data (*16*) reveal that a warming over the past 2 decades in the upper 900 m can be attributed to a wind-induced thickening of the thermocline, whereas temperature and salinity changes in the deeper waters can be accounted for by changes in the water masses spreading from the Mediterranean and Labrador Seas.

Given the prominent role of the surface forcing, we explored whether the large-scale atmospheric variability, as expressed by the North Atlantic Oscillation (NAO) index, can impart the observed oceanic heat-content change. Within the 50-year span of our observations, there has been a well-recognized shift in the NAO from a low index from 1950 to 1970 to a high index from 1980 to 2000 (*17*). To address the role of this change in large-scale atmospheric forcing, we abandoned the integration of the model with sequential forcing and instead simply ran the model for a 20-year period with atmospheric forcing from a composite of NAO– years and for a 20-year period with a composite of NAO+ years. A computation of the model differences in heat content (Fig. 4 and fig. S3C) reveals that the NAO+ ocean has a larger heat content in the subtropics and tropics compared with the NAO– ocean, whereas the opposite is true for the subpolar region. Such a contrast matches the general pattern for the observed heat-content changes (Fig. 1A), as well as that for the difference between the two model runs forced with 1950–1970 conditions and 1980–2000 conditions (Fig. 1B). A comparison of the zonally integrated heat-content changes as a function of latitude (Fig. 4B) confirms that the NAO difference can largely account for the observed gyre-specific heat-content changes over the past 50 years, although there are some notable differences in the latitudinal band from 35° to 45°N. Thus, we suggest that the large-scale, decadal changes in wind and buoyancy forcing associated with the NAO is primarily responsible for the ocean heat-content changes in the North Atlantic over the past 50 years.

This data and modeling study of heat-content changes for the North Atlantic provides several cautionary notes for the investigation and interpretation of climate signals in the ocean. First, an examination of the spatial pattern associated with the reported heat-content changes illustrates that basin-averaged changes can mask important spatial differences. Secondly, there is not a single attribution for the observed changes in the North Atlantic heat content: Changes in surface buoyancy forcing lead to tropical warming and high-latitude cooling, whereas wind-induced redistribution of heat leads to subtropical warming. Thirdly, the broad pattern of heat-content change can be accounted for by changes in the large-scale atmospheric forcing over the past 50 years.

When viewed in isolation, the net heat gain for the North Atlantic basin (+0.4 W m^{-2}) is likely explained as a small residual from the cancellation of the larger regional heat gains and losses (±4 W m^{-2}). Any anthropogenic warming would presently be masked by such strong natural variability. However, given the reported heat gain for each of the other world ocean basins (*1*, *2*, *18*) and the rising air temperatures, the relatively small basinwide heat gain is plausibly attributable to anthropogenic forcing. The overall North Atlantic heat-content change, equivalent to an average increase in the surface heat flux of +0.4 W m^{-2}, is the same sign yet slightly below the lower estimates of anthropogenic-induced radiative heating, ranging from +0.6 to +2.4 W m^{-2} since 1750 (*19*). Presumably, other parts of the global ocean and climate system have taken up the remainder of the excess heat input.

Lastly, the positive trend in the winter NAO index in the 1990s has been attributed to anthropogenic forcing (*17*), implying that the NAO could be the route by which anthropogenic warming is imprinted on the ocean. However, although most climate models show a slight strengthening of the NAO index with anthropogenic forcing, the climate models also underestimate the strength of the recent decadal trend in the NAO, raising doubts as to the viability of the connection between the NAO and anthropogenic forcing in climate models (*20*, *21*). Hence, although the change in ocean heat content over the North Atlantic can be connected to the decadal trend in the NAO, it is premature to conclusively attribute these regional patterns of heat gain to greenhouse warming. Continued long-term monitoring of North Atlantic temperatures is needed to answer the question of whether the basin-average warming is reflecting anthropogenic forcing and/or natural variability.

References and Notes

1. S. Levitus, J. I. Antonov, T. P. Boyer, C. Stephens, *Science* **287**, 2225 (2000).
2. S. Levitus, J. I. Antonov, T. P. Boyer, *Geophys. Res. Lett.* **32**, L02604 (2005).
3. S. Levitus *et al.*, *Science* **292**, 267 (2001).
4. B. K. Arbic, W. B. Owens, *J. Clim.* **14**, 4091 (2001).
5. H. L. Bryden *et al.*, *J. Clim.* **9**, 3162 (1996).
6. T. M. Joyce, R. S. Pickart, R. C. Millard, *Deep Sea Res.* **46**, 245 (1999).
7. J. R. Lazier, in *Natural Climate Variability on Decade-to-Century Time Scales* (National Academy Press, Washington, DC, 1995), p. 295.
8. R. Curry, B. Dickson, I. Yashayaev, *Nature* **426**, 826 (2003).
9. M. S. Lozier, W. B. Owens, R. G. Curry, *Prog. Oceanogr.* **36**, 1 (1995).
10. T. P. Boyer *et al.*, *World Ocean Database 2005*, S. Levitus, Ed. (National Oceanic and Atmospheric Administration Atlas National Environmental Satellite, Data, and Information Service 60, Government Printing Office, Washington, DC, 2006).
11. R. Bleck, L. T. Smith, *J. Geophys. Res.* **95**, 3273 (1990).
12. S. M. Uppala *et al.*, *Q. J. R. Meteorol. Soc.* **131**, 2961 (2005).
13. E. Kalnay *et al.*, *Bull. Am. Meteorol. Soc.* **77**, 437 (1996).
14. N. L. Bindoff, T. J. McDougall, *J. Phys. Oceanogr.* **24**, 1137 (1994).
15. The decomposition is expressed mathematically as $\frac{\partial T}{\partial t}|_z = \frac{\partial T}{\partial t}|_\rho + \frac{\partial T}{\partial z}\frac{\partial z}{\partial t}|_\rho$.
16. S. J. Leadbetter, R. G. Williams, E. L. McDonagh, B. A. King, *Geophys. Res. Lett.* **34**, L12608 (2007).
17. J. W. Hurrell, *Science* **269**, 676 (1995).
18. N. L. Bindoff *et al.*, in *Climate Change 2007: The Physical Science Basis. Contribution of Working Group I to the Fourth Assessment Report of the Intergovernmental Panel on Climate Change*, S. Solomon *et al.*, Eds. (Cambridge Univ. Press, Cambridge, 2007).
19. P. Forster *et al.*, in *Climate Change 2007: The Physical Science Basis. Contribution of Working Group I to the Fourth Assessment Report of the Intergovernmental Panel on Climate Change*, S. Solomon *et al.* Eds. (Cambridge Univ. Press, Cambridge, 2007).
20. N. P. Gillett, H. F. Graf, T. J. Osborn, *Geophys. Monogr. Am. Geophys. Union 134* (American Geophysical Union, Washington, DC, 2003).
21. D. B. Stephenson *et al.*, *Clim. Dyn.* **27**, 401 (2006).

22. This work was supported by grants from NSF and the UK Natural Environment Research Council. Atmospheric data sets were obtained from the British Atmospheric Data Centre.

Supporting Online Material

www.sciencemag.org/cgi/content/full/1146436/DC1
Materials and Methods
Figs. S1 to S3
Table S1
References

13 June 2007; accepted 17 December 2007
Published online 3 January 2008;
10.1126/science.1146436
Include this information when citing this paper.

Downloaded from www.sciencemag.org on February 8, 2008

Supporting Online Material

Methods

Heat Content Calculation

Heat content change for each bin, ΔQ, was calculated using $\Delta Q = Q_{1980\text{-}2000} - Q_{1970\text{-}1950}$, where $Q_{1980-2000} = V(\overline{\rho}\,\overline{C_p}\,\overline{T})_{1980-2000}$; V is the volume of each bin and $\overline{\rho}$, $\overline{C_p}$, and $\overline{T}$ denote the mean density, specific heat capacity and temperature, respectively, that result from averaging all data in a bin over the time period 1980-2000. $Q_{1970\text{-}1950}$ was calculated similarly, but with data over the time period 1950-1970. The depth-integrated heat content change was calculated as the sum of the heat content changes for the eleven contiguous layers that extend from the sea surface to near the sea floor. This analysis used 65,275 hydrographic stations from 1950-1970 and 98,178 hydrographic stations from 1980-2000. Results using two contiguous time periods (1950-1975 and 1976-2000) yielded similar results.

Model formulation

An isopycnic model (MICOM 2.7; *S1*) was integrated at 1.4^{o} resolution on a Mercator grid over the North Atlantic with 15 potential density layers (referenced to the sea surface) plus a surface mixed layer with variable density. The model was initialized from climatology with a topography based on ETOP05 data and then integrated from rest for 60 years using climatological monthly wind stresses, surface heat and freshwater fluxes from weather reanalyses together with precipitation data *(S2, S3)*. Two spin-ups were made: one using monthly ECMWF (ERA40) forcing fields averaged from 1958 to 2000; the other using monthly NCEP forcing fields averaged from 1950 to 2000. The surface heat and freshwater forcing includes a weak relaxation on an annual timescale to monthly mean surface temperature and salinity over the domain to avoid long-term drift. River runoff was included by a surface, freshwater input and the effect of the Mediterranean Sea was simulated by relaxing salinity over the full depth in grid cells adjacent to the Straits of Gibraltar. The model domain extends from 64^{o}N to 35^{o}S with salinity and isopycnal layer depth relaxed towards climatology over a buffer zone south of the equator. After the spin up, the modeled surface temperature agrees reasonably well with climatology: the Gulf Stream separates from the coast just north of Cape Hatteras, and there is a realistic thermocline structure, with thickening over the subtropical gyres and thinning over the equator and subpolar gyre (Fig. S2). However, as with other models with similar resolution, the Gulf Stream is displaced too far to the north, a mismatch unlikely to impact our results.

Supplementary Figure 1

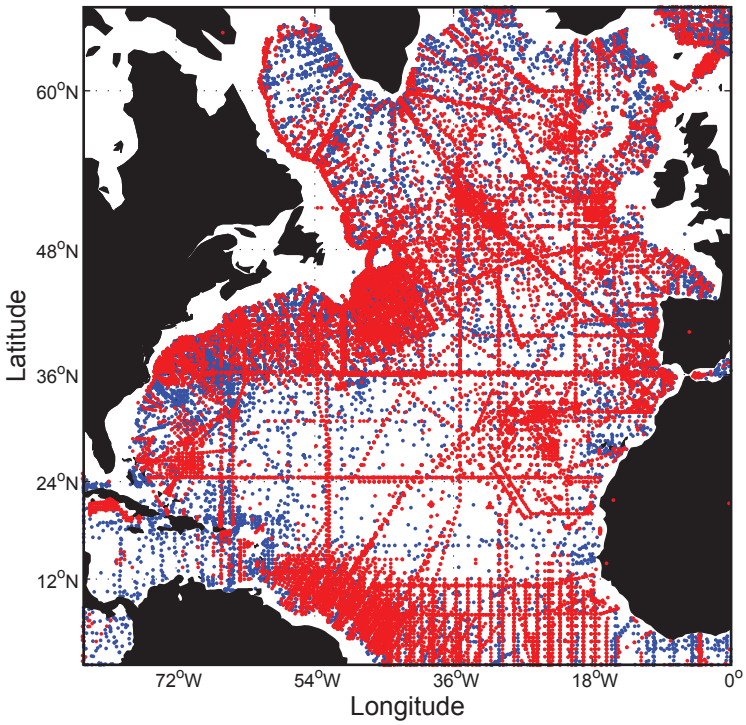

Figure S1: Distribution of observations from historical hydrographic stations used to diagnose the heat content change for two 20-year periods: 1980-2000 (red) and 1950-1970 (blue).

Supplementary Figure 2

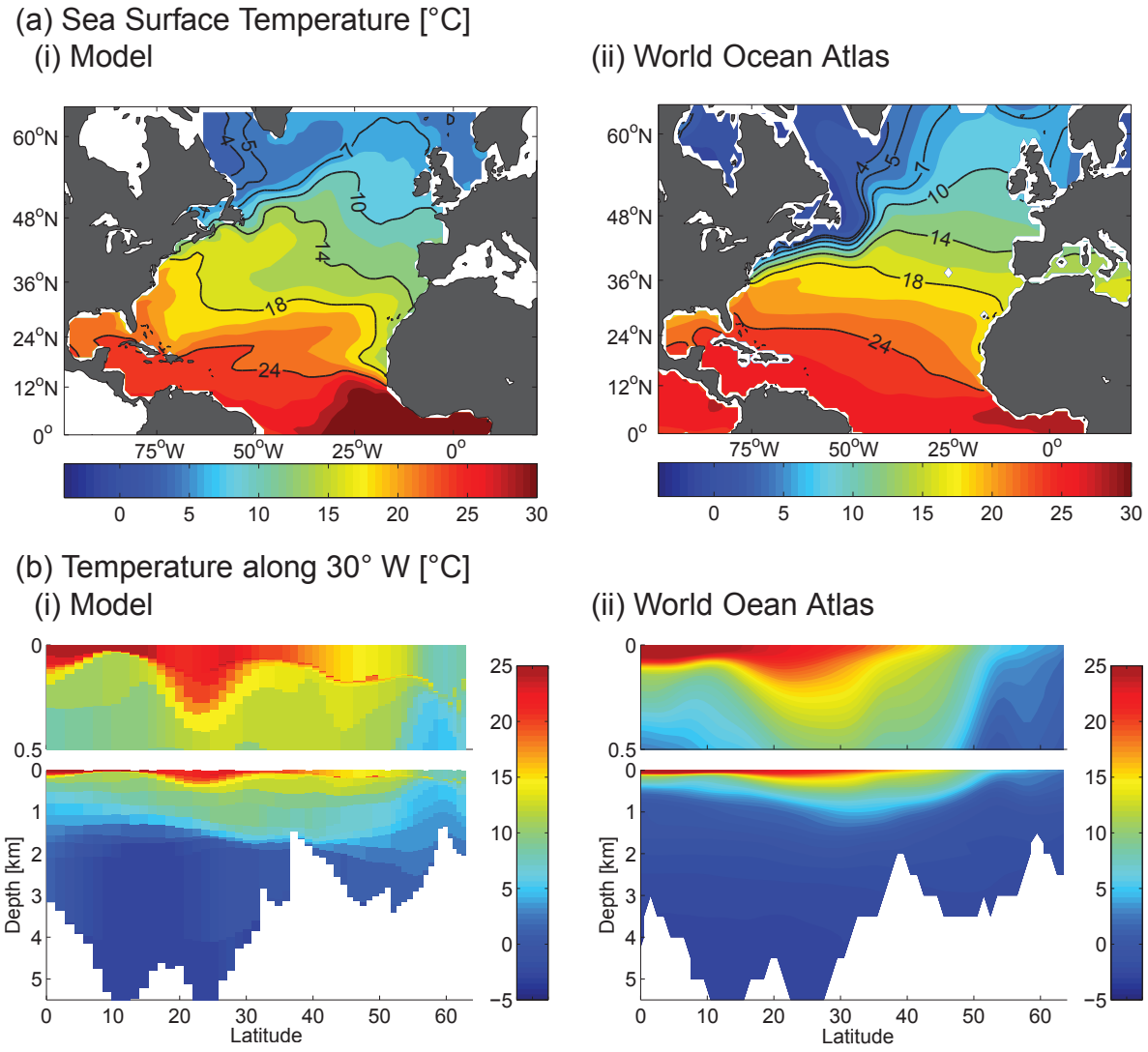

Figure S2: (a) Map of sea surface temperature (˚C) at the end of winter and (b) a meridional section of temperature (˚C) along 30oW from the (i) model climatology after 60 years integration and (ii) climatological data.

Supplementary Figure 3

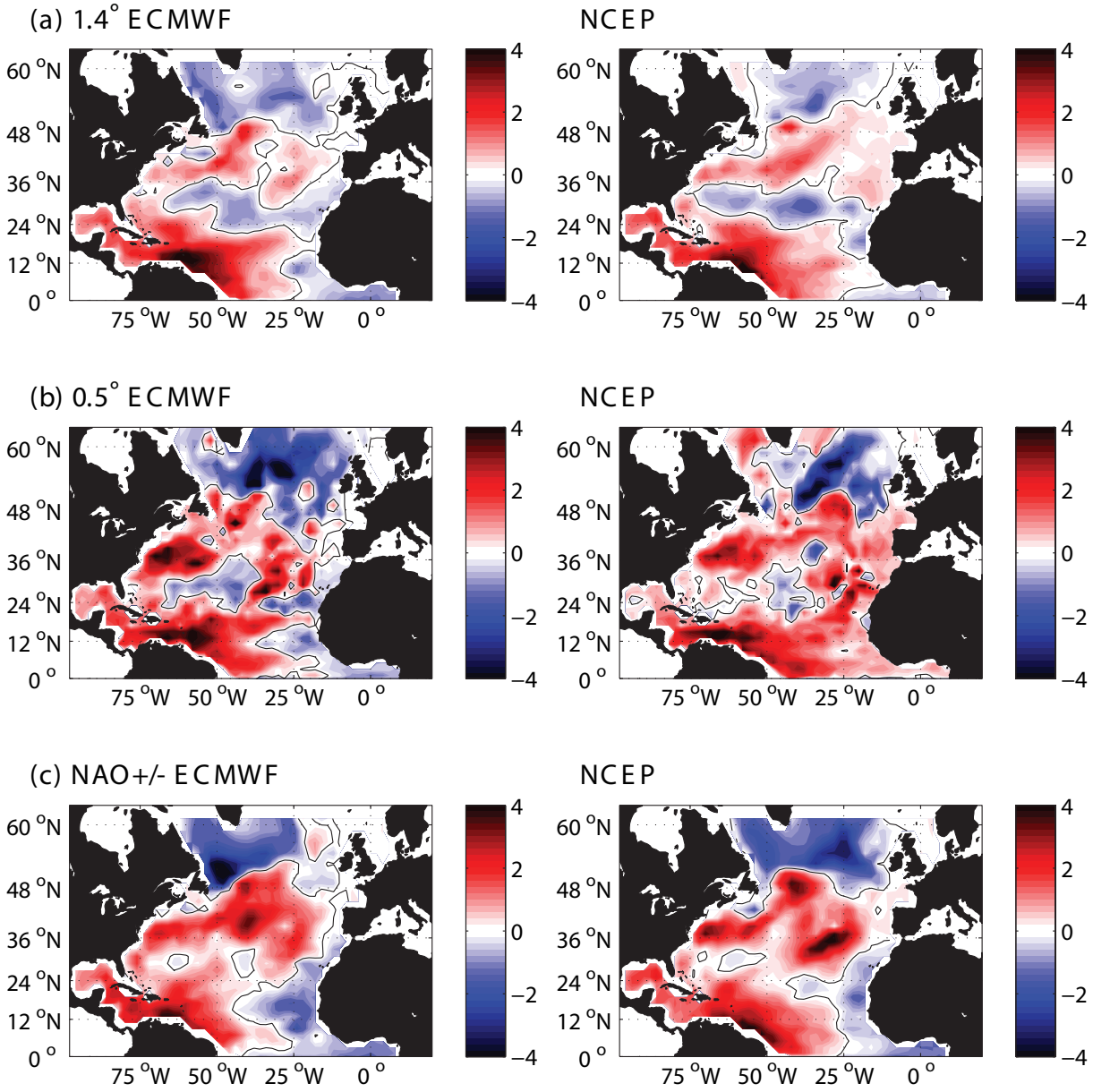

Figure S3: Change in ocean heat content (10^{20} J; red is a gain) between model experiments for 1980-2000 and 1950-1970 using surface forcing derived from ECMWF and NCEP re-analysis data (left and right panels, respectively) after a 60-year spin up: (a) 1.4˚ resolution model; (b) 0.5˚ resolution model; (c) idealized case where the model difference is based on the experiment with NAO+ forcing versus NAO- forcing for a 1.4˚ model. While the details of the model results differ, all cases show a broad resemblance to the observations with a heat gain in the tropics and subtropics, and a loss in the subpolar ocean.

Table S1: Integrated heat content change between 1980-2000 and 1950-1970 for the North Atlantic from observations and model experiments				
	Heat Content Change [10^{22} J]			
	1-19°N	**21-49°N**	**51-63°N**	**1-63°N**
Observed changes	1.27± .07	1.39±.16	-1.05±.06	1.61±.19
Modeled changes				
ECMWF forcing at 1.4º resolution	3.01	1.18	-0.91	3.28
NCEP forcing at 1.4º resolution	2.83	1.41	-0.43	3.81
Idealized experiment with realistic buoyancy fluxes and climatological winds (based upon ECMWF)	1.31	0.02	-0.63	0.70
Idealized experiment with climatological buoyancy fluxes and realistic winds (based upon ECMWF)	1.47	2.18	-0.10	3.55
Idealized experiment with NAO+ minus NAO- states (based upon ECMWF)	1.27	3.66	-1.37	3.56

References

S1. R. Bleck and L. Smith, *J. Geophys. Res.*, **95**, 3273 (1990).

S2. A. M. da Silva, C. C. Young, and S. Levitus, *Atlas of Surface Marine Data 1994. Vol. 1: Algorithms and Procedures. NOAA Atlas NESDIS.* (1994) [Obtained from the LDEO/IRI Data Library at http://ingrid.ldgo.columbia.edu/SOURCES/.DASILVA/.SMD94/.climatology/ (2005)].

S3. G. J. Huffman *et al., Bull. Am. Meteorol. Soc.* **78,** 5 (1997). [NASA Global Climatology Precipitation Project - Version 2. Obtained from the LDEO/IRI Data Library at http://iridl.ldeo.columbia.edu/SOURCES/.NASA/.GPCP/.V2/ (2005)]